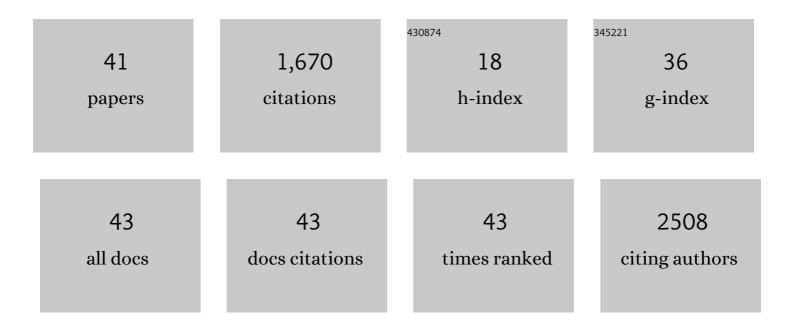
Soo-Ghang Ihn

List of Publications by Year in descending order

Source: https://exaly.com/author-pdf/7819054/publications.pdf Version: 2024-02-01



#	Article	IF	CITATIONS
1	Dipole Moment―and Molecular Orbitalâ€Engineered Phosphine Oxideâ€Free Host Materials for Efficient and Stable Blue Thermally Activated Delayed Fluorescence. Advanced Science, 2022, 9, e2102141.	11.2	21
2	Designing Stable Deepâ€Blue Thermally Activated Delayed Fluorescence Emitters through Controlling the Intrinsic Stability of Triplet Excitons. Advanced Optical Materials, 2022, 10, .	7.3	7
3	Designing Stable Deepâ€Blue Thermally Activated Delayed Fluorescence Emitters through Controlling the Intrinsic Stability of Triplet Excitons (Advanced Optical Materials 12/2022). Advanced Optical Materials, 2022, 10, .	7.3	0
4	High-efficiency, long-lifetime deep-blue organic light-emitting diodes. Nature Photonics, 2021, 15, 208-215.	31.4	335
5	Improved Efficiency and Lifetime of Deepâ€Blue Hyperfluorescent Organic Lightâ€Emitting Diode using Pt(II) Complex as Phosphorescent Sensitizer. Advanced Science, 2021, 8, e2100586.	11.2	91
6	Cohosts with efficient host-to-emitter energy transfer for stable blue phosphorescent organic light-emitting diodes. Journal of Materials Chemistry C, 2021, 9, 17412-17418.	5.5	7
7	Improved Efficiency and Stability of Blue Phosphorescent Organic Light Emitting Diodes by Enhanced Orientation of Homoleptic Cyclometalated Ir(III) Complexes. Advanced Optical Materials, 2020, 8, 2001103.	7.3	24
8	Direct characterization of vertical molecular distributions of organic bulk heterojunction structure by photoemission spectroscopy combined with argon gas cluster ion beam sputtering. Applied Surface Science, 2020, 515, 146102.	6.1	6
9	Charge Recombination in Polaron Pairs: A Key Factor for Operational Stability of Blueâ€Phosphorescent Lightâ€Emitting Devices. Advanced Theory and Simulations, 2020, 3, 2000028.	2.8	6
10	Blue Electroluminescence: Blue Electrofluorescence Resulting from Exergonic Harvesting of Triplet Excitons (Advanced Optical Materials 18/2019). Advanced Optical Materials, 2019, 7, 1970070.	7.3	0
11	High-efficiency blue organic light-emitting Diodes using emissive carbazole-triazine-based donor-acceptor molecules with high reverse intersystem crossing rates. Organic Electronics, 2019, 75, 105399.	2.6	6
12	Blue Electrofluorescence Resulting from Exergonic Harvesting of Triplet Excitons. Advanced Optical Materials, 2019, 7, 1900630.	7.3	10
13	A Novel Design Strategy for Suppressing Efficiency Roll-Off of Blue Thermally Activated Delayed Fluorescence Molecules through Donor–Acceptor Interlocking by C–C Bonds. Nanomaterials, 2019, 9, 1735.	4.1	7
14	Molecular Design of Deep Blue Thermally Activated Delayed Fluorescence Materials Employing a Homoconjugative Triptycene Scaffold and Dihedral Angle Tuning. Chemistry of Materials, 2018, 30, 1462-1466.	6.7	71
15	Degradation of blue-phosphorescent organic light-emitting devices involves exciton-induced generation of polaron pair within emitting layers. Nature Communications, 2018, 9, 1211.	12.8	107
16	An Alternative Host Material for Longâ€Lifespan Blue Organic Lightâ€Emitting Diodes Using Thermally Activated Delayed Fluorescence. Advanced Science, 2017, 4, 1600502.	11.2	103
17	3D reconstruction modeling of bulk heterojunction organic photovoltaic cells: Effect of the complexity of the boundary on the morphology. Journal of the Korean Physical Society, 2016, 68, 474-481.	0.7	0
18	Auger electron nanoscale mapping and x-ray photoelectron spectroscopy combined with gas cluster ion beam sputtering to study an organic bulk heterojunction. Applied Physics Letters, 2014, 104, 243303.	3.3	6

SOO-GHANG IHN

#	Article	IF	CITATIONS
19	Enhancement of the power conversion efficiency in a polymer solar cell using a work-function-controlled TimSinOx interlayer. Journal of Materials Chemistry A, 2014, 2, 2033-2039.	10.3	4
20	Autocatalytic effect of amine-terminated precursors in mixed self-assembled monolayers. RSC Advances, 2013, 3, 1112-1118.	3.6	5
21	Controlled nanomorphology of PCDTBT–fullerene blends via polymer end-group functionalization for high efficiency organic solar cells. Chemical Communications, 2012, 48, 7206.	4.1	49
22	Synthesis and photovoltaic properties of benzo[1,2-b:4,5-bâ€2]dithiophene derivative-based polymers with deep HOMO levels. Journal of Materials Chemistry, 2012, 22, 17709.	6.7	31
23	Controlling band gap and hole mobility of photovoltaic donor polymers with terpolymer system. Polymer, 2012, 53, 5275-5284.	3.8	16
24	Control of naturally coupled piezoelectric and photovoltaic properties for multi-type energy scavengers. Energy and Environmental Science, 2011, 4, 4607.	30.8	51
25	Low-temperature growth and characterization of ZnO thin films for flexible inverted organic solar cells. Journal of Materials Chemistry, 2011, 21, 12274.	6.7	26
26	High Performance Organic Photovoltaic Cells Using Polymerâ€Hybridized ZnO Nanocrystals as a Cathode Interlayer. Advanced Energy Materials, 2011, 1, 690-698.	19.5	123
27	ITO-free inverted polymer solar cells using a GZO cathode modified by ZnO. Solar Energy Materials and Solar Cells, 2011, 95, 1610-1614.	6.2	52
28	Enhanced Performance in Polymer Solar Cells by Surface Energy Control. Advanced Functional Materials, 2010, 20, 4381-4387.	14.9	250
29	Optical properties of undoped, Be-doped, and Si-doped wurtzite-rich GaAs nanowires grown on Si substrates by molecular beam epitaxy. Solid State Communications, 2010, 150, 729-733.	1.9	27
30	Density Control of ZnO Nanorod Arrays on Mixed Self-Assembled Monolayers. Crystal Growth and Design, 2010, 10, 4697-4700.	3.0	6
31	InAs nanowires on Si substrates grown by solid source molecular beam epitaxy. Nanotechnology, 2007, 18, 355603.	2.6	41
32	Growth of GaAs Nanowires on Si Substrates Using a Molecular Beam Epitaxy. IEEE Nanotechnology Magazine, 2007, 6, 384-389.	2.0	32
33	Morphology- and Orientation-Controlled Gallium Arsenide Nanowires on Silicon Substrates. Nano Letters, 2007, 7, 39-44.	9.1	99
34	Molecular beam epitaxy growth of In0.52Al0.48Asâ^•In0.53Ga0.47As metamorphic high electron mobility transistor employing growth interruption and in situ rapid thermal annealing. Applied Physics Letters, 2006, 88, 132108.	3.3	9
35	Effects of Beryllium Doping into InGaAlAs Metamorphic Buffer on High-Electron-Mobility Transistor Structure. Japanese Journal of Applied Physics, 2006, 45, 724-726.	1.5	3
36	GaAs nanowires on Si substrates grown by a solid source molecular beam epitaxy. Applied Physics Letters, 2006, 89, 053106.	3.3	31

#	Article	IF	CITATIONS
37	Carrier dynamics of low-temperature-grown In0.53Ga0.47As on GaAs using an InGaAlAs metamorphic buffer. Applied Physics Letters, 2005, 86, 111903.	3.3	3
38	Effects of postgrowth rapid thermal annealing on InAlAsâ^•InGaAs metamorphic high-electron-mobility transistor grown on a compositionally graded InAlAsâ^•InGaAlAs buffer. Applied Physics Letters, 2005, 87, 042108.	3.3	2
39	Effects of rapid thermal annealing on quality of In0.52Al0.48Asâ^•In0.53Ga0.47As multiquantum wells grown on a compositionally graded InAlAsâ^•InAlGaAs metamorphic buffer layer. Applied Physics Letters, 2004, 85, 6335-6337.	3.3	3
40	Crystalline quality improvement of In/sub 0.52/Al/sub 0.48/As/In/sub 0.53/Ga/sub 0.37/As heterostructure on InAlAs/InGaAlAs/GaAs metamorphic buffer by post-growth rapid thermal annealing. , 0, , .		0
41	Carrier lifetime of low-temperautre-grown In/sub 0.53/ga/sub 0.47/as on GaAs using an InGaAlAs metamorphic buffer. , 0, , .		0